Magnetic Resonance Elastography of the Hippocampal Subfields in Alzheimer's Disease

Lucy V Hiscox[1,2], Curtis L Johnson[2], Matthew DJ McGarry[3], Helen Marshall[1], Edwin JR van Beek[1], Neil Roberts[1], and John M Starr[1]

[1]University of Edinburgh, Edinburgh, United Kingdom, [2]University of Delaware, Newark, DE, United States, [3]Dartmouth College, Hanover, NH, United States

Synopsis

Magnetic resonance elastography (MRE) of the hippocampus has shown promise as an imaging biomarker for Alzheimer's disease (AD). In this work, we report that MRE of the hippocampal subfields are consistent with the known cytoarchitecture. We also found softening of the hippocampal subfields in patients with AD compared to healthy controls with a more pronounced reduction in the subiculum and CA1 compared to the global hippocampus. The dentate-gyrus/CA3 was also more viscoelastic in AD (indicating greater elasticity and less viscosity), whereas no viscoelastic effect was detected globally. MRE of the subfields may provide additional information regarding hippocampal integrity in disease.

Background

A focus of recent work in neuroimaging has been to establish new contrast mechanisms for detecting brain pathologies. Magnetic resonance elastography (MRE) enables measurement of tissue viscoelasticity[1] which is sensitive to microstructural tissue health[2]. Correlations have been reported between hippocampal viscoelasticity and memory performance[3,4] and reduction in viscoelasticity in AD patients[5]. To date, these studies have focused on the hippocampal formation as a whole. However, the hippocampus comprises several structurally- and functionally-distinct subfields (HCsf), which an *ex vivo* study of the rat hippocampus has shown vary in their mechanical properties[6]. Accordingly, alterations in the cell type, size, and configuration of neurons are expected to influence MRE-derived measurements of viscoelasticity. Since the HCsf also exhibit differential sensitivity to disease[7] measurement of their viscoelasticity could provide greater specificity for differentiating between healthy controls and AD patients.

Aims

To utilize recent developments in high-resolution MRE and improvements in automatic MR image segmentation to measure the mechanical properties of the individual HCsf in cognitively healthy older adults (OA) and patients with AD. First, we will investigate whether the mechanical properties of each subfield (to include the subiculum [parasubiculum, presubiculum, subiculum], cornu ammonis 1 [CA1], and the combined dentate gyrus-CA3 [DG-CA3]) are consistent with known cytoarchitecture. Second, the mechanical properties of the HCsf will be compared in OA controls and AD patients.

Methods

Twelve OA controls (mean age: 69.4+2.3 years, 6F/6M) and ten patients with AD (mean age: 77.1+5.8 years, 6F/4M) were recruited from the memory clinic at the Weston General Hospital, the Centre for Dementia Prevention in Edinburgh, and the Joint Dementia Research database. Mean scores for the Montreal Cognitive Assessment were: AD = 18.4; OA = 28.1. MRE data were acquired at 1.6 mm isotropic resolution using a 3D multishot, multislab spiral MRE sequence[8] and inverted with the nonlinear inversion (NLI) algorithm incorporating soft prior regularization (SPR)[9]. MRE data quality was measured by OSS-SNR[10]. Masks of the whole HC and the HCsf were obtained via automatic segmentation of corresponding T_1-weighted images using Freesurfer v. 6.0 through the recon-all and additional subfield pipelines. FLIRT within FSL was used to co-register the individual HC and HCsf masks into MRE space. The SPR inversions considered the whole HC and each HCsf separately. Outcome measures were shear stiffness, μ, and damping ratio, ξ.

Results

Differentiation of subfield viscoelasticity

A one-way ANOVA and Tukey post-hoc comparisons were performed to analyze differences in HCsf mechanical properties within the OA and AD groups, as illustrated in Figure 1. In both groups, the subiculum was significantly stiffer than the DG-CA3. In the AD group, the subiculum was also significantly stiffer than the CA1. ξ also varied between HCsf: in both groups subiculum ξ was significantly lower than DG-CA3 and CA1. Of interest and in contrast to OA, the DG-CA3 and CA1 did not differ from one another in AD.

OA vs. AD

In all regions the AD group exhibited lower stiffness: an independent samples *t*-test revealed the differences were significant for whole HC ($p = 0.018$), subiculum ($p = 0.002$), and CA1 ($p = 0.007$), whereas the difference in DG-CA3 approached significance ($p = 0.054$). For ξ a significant difference was detected in DG-CA3 only ($p = 0.026$), which was lower in AD. Mean values and effect sizes are displayed in Figure 2. Example images of each subfield for OA and AD are presented in Figures 3 and 4.

Conclusions

We have demonstrated the viability of performing MRE of HCsf and have detected differences in their mechanical properties that is consistent with known cytoarchitecture. The subiculum was found to exhibit greater viscoelasticity (i.e. lower ξ) which may be due to the crude organization of small pyramidal cells, which is in contrast to the diffuse organization of neurons within the CA1. We also found that the hippocampus is softer in AD patients, and that this

effect is more pronounced in the subiculum and CA1. Interestingly, no difference in ξ was found within the HC globally; however, lower ξ was detected within the DG-CA3 indicating greater elasticity and less viscosity that is suggestive of more cells and connections. We hypothesise this may be related to neuroproliferation in DG, which is known to be enhanced in AD[11]. While more neurons may be generated, they are less likely to reach maturity, which may explain the lower DG-CA3 stiffness reported. Future work will assess HCsf viscoelasticity in patients with mild cognitive impairment that may assist in the early detection of those at risk of AD.

Acknowledgements

Funding from the Alzheimer Scotland Dementia Research Centre and National Institutes of Health (R01-AG058853) is gratefully acknowledged.

References

[1] Muthupillai R, Lomas, DJ, Rossman PJ, et al. Magnetic resonance elastography by direct visualization of propagating acoustic strain waves. Science. 1995; 269:1854–1857.

[2] Sack I, Jöhrens K, Würfel J et al. Structure-sensitive elastography: on the viscoelastic powerlaw behavior of in vivo human tissue in health and disease. Soft Matter. 2013; 9, 5672.

[3] Schwarb H, Johnson CL, McGarry MDJ, et al. Medial temporal lobe viscoelasticity and relational memory performance. NeuroImage. 2016;132: 534-41.

[4] Hiscox LV, Johnson CL, McGarry MDJ et al. Hippocampal viscoelasticity and episodic memory performance in healthy older adults examined with magnetic resonance elastography. Brain Imaging Behav. 2018; doi: 10.1007/s11682-018-9988-8.

[5] Gerischer LM, Fehlner A, Köbe T, et al. Combining viscoelasticity, diffusivity and volume of the hippocampus for the diagnosis of Alzheimer's disease based on magnetic resonance imaging. Neuroimage Clin. 2017; 18:485-493.

[6] Elkin BS, Azeloglu EU, Costa KD, et al. Mechanical Heterogeneity of the Rat Hippocampus Measured by Atomic Force Microscope Indentation. J. Neurotrauma. 2007; 24, 812–822.

[7] Small SA, Schobel SA, Buxton RB, et al., A pathophysiological framework of hippocampal dysfunction in ageing and disease. Nat Rev Neurosci. 2011; 12: 585–601.

[8] Johnson CL, Holtrop JL, McGarry MDJ, et al. 3D multislab, multishot acquisition for fast, whole-brain MR elastography with high signal-to-noise efficiency. Magn Reson Med. 2014;71: 477–485.

[9] McGarry MDJ, Johnson CL, Sutton BP, et al. Including spatial information in nonlinear inversion MR elastography using soft prior regularization. IEEE Trans Med Imaging. 2013;32: 1901–1909.

[10] McGarry MDJ, Van Houten EEW, Perrinez PR, et al. An octahedral shear strain-based measure of SNR for 3D MR elastography. Phys Med Biol. 2011; 56: 153–64.

[11] Li B, Yamamori H, Tatebayashi Y, et al. Failure of neuronal maturation in Alzheimer disease dentate gyrus. J. Neuropathol. Exp. Neurol. 2008; 67, 78-84.

Figures

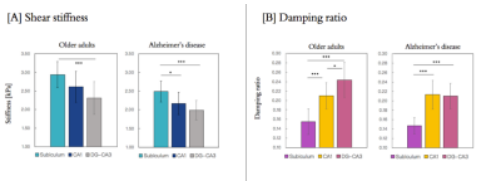

Figure 1. Mean MRE values of (A) shear stiffness and (B) damping ratio, according to HCsf region and diagnostic group (OA = older adults; AD = Alzheimer's disease). Graphs illustrate mean and standard deviation. * = $p < 0.05$, *** = $p < 0.001$.

	OA	AD	T-test	Cohen's *d*	% difference
Shear stiffness μ (kPa)					
Hippocampus	2.60 (0.33)	2.27 (0.24)	**$p = 0.018$**	**1.14**	**-12.7%**
Subiculum	2.94 (0.35)	2.49 (0.26)	**$p = 0.002$**	**1.46**	**-15.0%**
CA1	2.61 (0.42)	2.16 (0.28)	**$p = 0.007$**	**1.25**	**-17.2%**
DG-CA3	2.31 (0.44)	2.00 (0.25)	$p = 0.054$	0.86	-13.4%
Damping ratio ξ					
Hippocampus	0.201 (0.023)	0.202 (0.045)	$p = 0.910$	0.03	-0.5%
Subiculum	0.155 (0.027)	0.147 (0.017)	$p = 0.440$	0.35	-5.2%
CA1	0.210 (0.028)	0.213 (0.031)	$p = 0.800$	0.10	+1.4%
DG-CA3	0.244 (0.037)	0.210 (0.027)	**$p = 0.026$**	**1.05**	**-13.9%**

Figure 2. Summary statistics for each group in hippocampus and each hippocampal subfield.

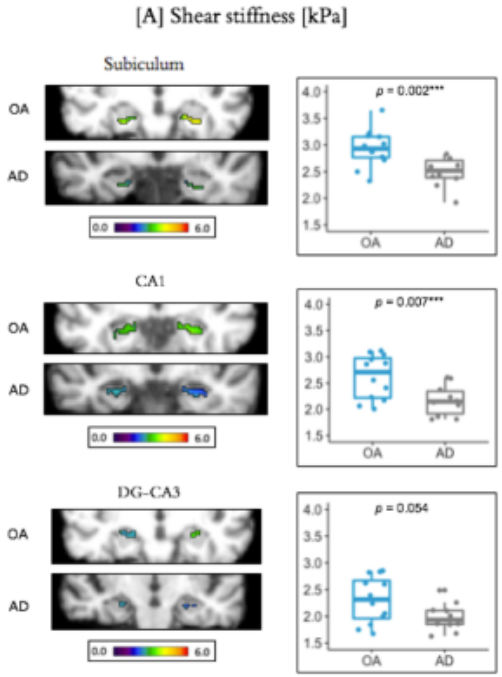

Figure 3. Example shear stiffness, μ maps of the HCsf in MRE native space. Graphs show the differences between older adults (OA) and patients with Alzheimer's disease (AD). *p* values represent results from an independent samples *t* test.

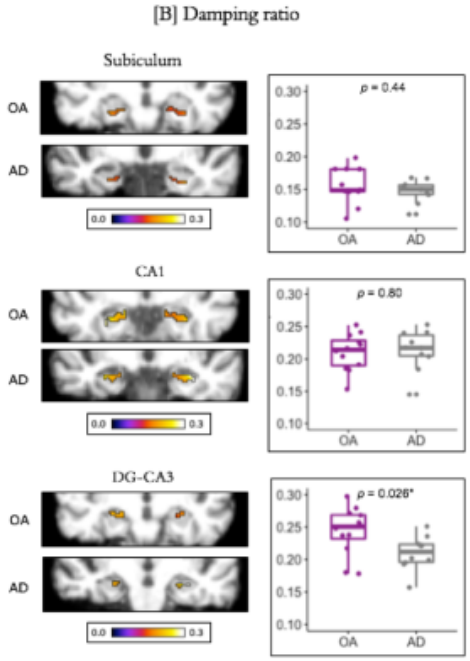

Figure 4. Example damping ratio, ξ maps of the HCsf in MRE native space. Graphs show the differences between older adults (OA) and patients with Alzheimer's disease (AD). *p* values represent results from an independent samples *t* test.